# Potent cytotoxicity of the phosphatase inhibitor microcystin LR and microcystin analogues in OATP1B1- and OATP1B3-expressing HeLa cells

**Noel R. Monks, Shuqian Liu, Yongsheng Xu, Hui Yu, Adam S. Bendelow, and Jeffrey A. Moscow**

**Department of Pediatrics, University of Kentucky, Lexington, Kentucky**

## Abstract

**Microcystins are a family of cyclic peptides that are potent inhibitors of the protein phosphatase families PP1 and PP2A. Only three human proteins are thought to be able to mediate the hepatic uptake of microcystins (the organic anion-transporting polypeptides OATP1B1, OATP1B3, and OATP1A2), and the predominant hepatic expression of these transporters accounts for the liver-specific toxicity of microcystins. A significant obstacle in the study of microcystins as anticancer drugs is the requirement of specific transport proteins for cellular uptake. We report that OATP1B3 mRNA is up-regulated in non–small cell lung cancer tumors in comparison with normal control tissues. This finding led to the exploration of microcystins as potential anticancer agents. We have developed a HeLa cell model with functional OATP1B1 and OATP1B3 activity. Transiently transfected HeLa cells are over 1,000-fold more sensitive to microcystin LR than the vector-transfected control cells, showing that transporter expression imparts marked selectivity for microcystin cytotoxicity. In addition, microcystin analogues showed variable cytotoxicities in the OATP1B1- and OATP1B3-transfected cells, including two analogues with $IC_{50}$ values < 1 nmol/L. Cytotoxicity of microcystin analogues seems to correlate to the inhibition of PP2A in these cells and induces rapid cell death as seen by chromatin condensation and cell fragmentation. These studies show that microcystin-induced phosphatase inhibition results in potent cytotoxicity when microcystin compounds can gain intracellular access and are a potent novel class of therapeutic agents for tumors expressing these uptake proteins. [Mol Cancer Ther 2007;6(2):587–98]**

Received 8/15/06; revised 11/14/06; accepted 12/15/06.

**Grant support:** Kentucky Lung Cancer Research Program.

The costs of publication of this article were defrayed in part by the payment of page charges. This article must therefore be hereby marked *advertisement* in accordance with 18 U.S.C. Section 1734 solely to indicate this fact.

**Requests for reprints:** Noel R. Monks, Department of Pediatrics, University of Kentucky, Room J457, 740 S. Limestone, Lexington, KY 40502. Phone: 859-323-8298; Fax: 859-257-6048. E-mail: Noel.Monks@uky.edu



doi:10.1158/1535-7163.MCT-06-0500

## Introduction

Phosphorylation of intracellular proteins is a key mechanism in the regulation of signal transduction. Kinases, enzymes that catalyze protein phosphorylation, are mediators of the signal cascades that activate multiple pathways involving the governance of cell division and cell death. Phosphatases are enzymes that counter the activity of kinases and remove organic phosphates from their active sites on regulatory molecules, which generally cause cessation of the activation signals. The importance of protein phosphatases in cell biology is underscored by the estimation that these proteins constitute >1% of all of the proteins encoded in the human genome (1). Mammalian protein phosphatases have been placed into five subfamilies, designated PP1, PP2A, PP2B, PP5, and PP7 (reviewed in ref. 2).

Microcystins are naturally occurring inhibitors of PP1 and PP2A and are generally known as hepatotoxins that result from cyanobacterial contamination of water supplies. Structurally, microcystins are cyclic heptapeptides with the basic structure cyclo(D-Ala L-X-*erythro*-b-*methyl*-D-*iso*-ASP-L-Y-adda-D-*iso*-Glu-*N*-methyldehydro-Ala), where L-X and L-Y represent variable L-amino acids, and adda is the β-amino acid 3-amino-9-methoxy-2,6,8-trimethyl-10-phenyldeca-4,6-dienoic acid (3). The most commonly studied microcystin is microcystin LR, in which the two variable amino acids are leucine and arginine. The structures of at least 50 microcystin variants have been determined (4), differing almost exclusively in the two variable residues, which can be other L-amino acids in substitution for leucine and arginine. The variable nature of these compounds suggests that they may have a spectrum of biological effects, and that there are opportunities for combinatorial engineering of therapeutic microcystin compounds.

The specific hepatic toxicity of microcystins results from the restricted hepatic expression of the organic anion-transporting polypeptides OATP1B1, OATP1B3, and OATP1A2, which mediate the cellular uptake of microcystins. OATP1B1 and OATP1B3 transporters have previously been known as liver-specific transporters 1 and 2, respectively, in recognition of gene expression limited to the liver. The potential potency of microcystin toxins in cancer cells has been difficult to examine due to the absence of expression of these transporters in most cancer cell lines. However, there is evidence for the expression of these transporters in tumors. Western blot analyses have detected the expression of both OATP1B1 and OATP1B3 in hepatocellular carcinoma (5, 6). In addition, Abe et al. (7) have reported that OATP1B1 and OATP1B3 are expressed in a few cell lines created from liver, colon, and pancreatic

tumors, suggesting that there may be a wider distribution of transporter gene expression in tumors than in normal tissues. Our interest in microcystins as potential therapeutic molecules began with our finding that OATP1B3 mRNA is up-regulated in non–small cell lung cancer (NSCLC). Therefore, the anticancer potential of microcystin compounds might be exploited by targeting these compounds to tumors that are known to express OATP1B1 and OATP1B3.

Given that the microcystins are potent protein phosphatase inhibitors, they are likely to affect both cell cycling and apoptosis. PP1 and PP2A directly regulate the activity of proteins phosphorylated on serine or threonine residues. PP2A has been shown to regulate the activity of at least 50 protein kinases involved in critical aspects of the regulation of cell division and cell death, including protein kinase C (PKC), Akt, extracellular signal-regulated kinase (ERK), mitogen-activated protein kinase (MEK), IκB kinase, p38, and caspase-3 (8–10). Inhibition of PP2A (by okadaic acid) has been shown to increase the phosphorylation and subsequent activation of p53, leading to cell cycle arrest and apoptosis (11, 12). Recent studies have identified PP2A as a key regulator of BCL-2 (13). Pharmacologic inhibition or RNA interference knockdown of PP2A caused proteasomic degradation of phosphorylated BCL-2 and sensitized the cells to various cell death stimuli. Therefore, we hypothesized that tumor cells might be selectively sensitive to microcystin-induced phosphatase inhibition. To test this hypothesis, we transfected cancer cells with the drug transporters OATP1B1 and OATP1B3 to create *in vitro* models in which microcystins could gain intracellular access, and the potential cytotoxicity of microcystins in cancer cells could be assessed.

## Materials and Methods

### Reagents and Cell Culture

HeLa cervical adenocarcinoma cells were obtained from the American Type Culture Collection (Manassas, VA). DMEM containing Glutamax-I, fetal bovine serum, PBS (pH 7.2), and LipofectAMINE 2000 were purchased from Invitrogen (Carlsbad, CA). Lung tumor specimens and matched adjacent nonmalignant tissue pairs were obtained from the National Cancer Institute Cooperative Human Tissue Network (Columbus, OH). Normal liver cDNA was purchased from Biochain Institute, Inc. (Hayward, CA). Microcystins LR and YR were purchased from Sigma (St. Louis, MO). Microcystin LF, LW, RR, and okadaic acid were all purchased from Axxora, LLC (San Diego, CA). [$^{33}$P]ATP was purchased from Perkin-Elmer (Boston, MA). All other chemicals were purchased from Sigma.

### Transporter Gene Expression Analysis by Quantitative PCR

A protocol to screen anonymous lung tumor specimens for transporter gene expression was approved by the University of Kentucky Institutional Review Board. For each transporter gene, we identified a primer set using the program Oligo 4.0. In each case, we showed that the primers amplify a PCR product of expected length. Total RNA was extracted from normal lung tissue and paired lung cancer specimens and cell lines using the RNeasy kit (Qiagen, Valencia, CA) with an on-column DNase digestion. A total of 3 μg of RNA was used as a template for the first-strand cDNA synthesis using the ThermoScript reverse transcription-PCR system (Invitrogen, Carlsbad, CA) with Oligo(dT) as the primer and done according to the manufacturer's protocol. Quantitative real-time PCR was done using the SYBR Green PCR kit (Applied Biosystems, Foster City, CA) and the iCycler thermal cycler (Bio-Rad, Hercules, CA). Quantification was performed using iCycler analysis software. The fluorescence threshold was set above the baseline in the exponential phase of the PCR, and from this, the $C_t$ (threshold cycle) was calculated for each reaction. The number of cycles required to reach the threshold fluorescence is proportional to the amount target RNA in the sample. The relative expression levels of the target genes were determined by calculating the relative amounts of RNA from PCR standard curves (cDNA from liver, kidney, or placenta was used as standards for the lung tissue expression analysis; plasmid DNA was used to for the cell line expression analysis) followed by normalization to the endogenous reference gene *β-actin*. All PCR products of the samples displayed a single, sharply melting curve with a narrow peak. Both *OATP1B1* and *OATP1B3* share >80% homology at the nucleotide level; therefore, primer specificity was confirmed by the inclusion of a negative control to each analysis (plasmid containing the alternative gene). Neither of the primer sets amplified the other gene.

### Transient Expression of OATP1B1 and OATP1B3

*OATP1B1* and *OATP1B3* cDNAs inserted into the multiple cloning site of the vector pIRESneo2 were obtained from Drs. Meier and Hagenbuch at the University of Zurich, and the nucleotide sequences of the coding regions were confirmed by nucleic acid sequencing.

Exponentially growing HeLa cells were seeded at $2 \times 10^5$ per well in six-well plates in 2 mL of DMEM supplemented with 5% FCS (without antibiotics). The cells were transfected 24 h later using LipofectAMINE 2000 (Invitrogen) at a ratio of lipid/DNA of 2:1 (2 μL/1 μg). In short, 2 μL of LipofectAMINE 2000 was diluted into 200 μL of Opti-MEM (Invitrogen); at the same time, 1 μg of plasmid DNA is also diluted into 200 μL of Opti-MEM and left to equilibrate for 5 min. The DNA and LipofectAMINE 2000 dilutions were mixed by pipetting, and complexes were allowed to form for 25 min. During complex formation, the cells were washed once with 37°C PBS, and 600 μL of DMEM supplemented with 5% FCS was added to each well. After 25 min, the complex mixture (400 μL) was carefully added to the cells and mixed gently, and transfection was allowed to proceed at 37°C, in 5% $CO_2$ for 4 h. After 4 h, 1 mL of DMEM supplemented with 10% FCS was added to each well, and the cells were returned to the incubator.

### Western Blot Analysis

Cells were washed twice in ice-cold PBS, lysed without trypsinization for 10 min at 4°C using a lysis buffer containing 150 mmol/L NaCl, 50 mmol/L Tris-HCl (pH 8),

1% NP40, 0.5% sodium deoxycholate, 0.1% SDS, and 0.02% sodium azide and 80 μL/mL of Complete Protease Inhibitor cocktail (Roche Applied Science, Indianapolis, IN). Samples were passed through a 25-gauge needle 10 times, and the lysate were collected following centrifugation at 12,000 × *g* for 5 min at 4°C. Protein concentrations were determined using the Bio-Rad *DC* protein assay (Bio-Rad). Equal amount of protein (25 μg per lane) were separated by 10% SDS-PAGE and subsequently transferred to PROTRAN BA85 nitrocellulose membrane (Whatman, Inc., Sanford, ME). The membranes were incubated with antibodies against PP1 and PP2A (Santa Cruz Biotechnology, Inc., Santa Cruz, CA) in 5% nonfat milk. After washing with TBS-Tween, the membranes were incubated with peroxidase-conjugated goat anti-mouse or goat anti-rabbit antibody (Jackson ImmunoResearch Laboratories, Inc., West Grove, PA) in 5% nonfat milk, followed by visualization using the enhanced chemiluminescence system (Amersham Biosciences, Piscataway, NJ). β-Actin (Sigma) was used to confirm equal protein loading.

### Drug Uptake Studies

Exponentially growing HeLa cells were transiently transfected with the plasmids containing *OATP1B1, OATP1B3,* or empty pIRESneo2 as described above. Forty-eight hours after transfection, the cells were exposed to two commercially available, radiolabeled substrates in uptake buffer [142 mmol/L NaCl, 5 mmol/L KCl, 1 mmol/L $K_2HPO_4$, 1.2 mmol/L $MgSO_4$, 1.5 mmol/L $CaCl_2$, 5 mmol/L glucose, and 12.5 mmol/L HEPES (pH 7.3)]: [$^3$H]BQ123 (Amersham Biosciences) for 30 min (final concentration, 0.5 μmol/L), a substrate for both transporters (14), and [$^3$H]cholecystokinin octapeptide (Amersham Biosciences) for 10 min (5 nmol/L), a substrate specific for the OATP1B3 transporter (14). The uptake assay was terminated by aspiration of the medium and three successive washes with ice-cold PBS. The cells were air-dried and solubilized by overnight incubation in 0.2 N NaOH followed by neutralization with 0.2 N HCl. The amount of intracellular radioactivity in the lysates was determined by liquid scintillation counting. The results were calculated by the subtraction of time 0 counts followed by normalization to the amount of cellular protein present in the lysates, which was determined spectrophotometrically using the Bio-Rad protein assay. Inhibition of transport was done by coincubation with 50 μmol/L bromosulfophthalein (Sigma).

### Growth Inhibition Studies

Cells were taken 24 h following transfection and seeded into 96-well plates at $1 \times 10^4$ per mL ($1 \times 10^3$ per well) and allowed to adhere for a further 24 h before drug treatments. The cells were then exposed to serial dilutions of the microcystin analogues prepared in culture medium for 72 h. For experiments in which cells were exposed to microcystin LR for 1 and 6 h, the media was carefully aspirated from the wells and replaced with 200 μL of fresh media. Cellular growth was determined using the sulforhodamine B protein dye assay (15). In short, cells were fixed with 50% trichloroacetic acid w/v (50 μL per well) for 1 h at 4°C. Following fixation, the plates were washed five to six times in water and stained with sulforhodamine B [0.4% sulforhodamine B (w/v) in 1% (v/v) acetic acid] for 30 min at 37°C. Excess stain was removed by washing five times in 1% (v/v) acetic acid. The plates were subsequently air-dried, and the protein-bound sulforhodamine B was re-solubilized by the addition of 10 mmol/L Trizma Base (pH 10.5). Colorimetric readings were made at 570 nm. $IC_{50}$ was calculated from the dose-response curve as the concentration of drug that produced a 50% decrease in the mean absorbance compared with the untreated wells.

### Clonogenic Survival Studies

HeLa cells were transiently transfected with *OATP1B1, OATP1B3,* or empty pIRESneo2 as described above. Forty-eight hours after transfection, cells were seeded into 60-mm culture dishes at 200 per dish in 5 mL of media. Six hours after seeding, microcystin LR was added to duplicate dishes and left for a further 72 h. Following microcystin LR exposure, the medium was carefully aspirated from the dishes and replaced with 5 mL of fresh media. The dishes were left for ~7 days until colonies were visible, at which time the cells were washed once with PBS, fixed using Carnoy's Fixative (methanol/acetic acid, 3:1) for 5 min, and stained using 0.4% crystal violet dissolved in water. The number of colonies on each plate was counted by eye, and survival was calculated as the percentage of control. $LC_{50}$ was extrapolated from the graph and is defined as the concentration at which the number of colonies was 50% of the control. The cloning efficiency is each transfected cell line was >95%.

### Inhibition of Purified Protein Phosphatases

Phosphatase activity was determined using the Protein Serine/Threonine Phosphatase Assay System (New England BioLabs, Inc., Beverly, MA). The *in vitro* activity of purified PP1 (New England Biolabs) and PP2A (Upstate Cell Signaling Solutions, Lake Placid, NY) was assayed according to the manufacturer's instructions. Briefly, PP1 or PP2A were diluted in phosphatase assay buffer [50 mmol/L Tris-HCl (pH 7.5), 0.1 mmol/L $Na_2EDTA$, 5 mmol/L DTT, and 0.01% Brij 35] at a concentration where the enzyme concentration is linear with dephosphorylation (≈30%) of the [$^{33}$P]ATP-labeled myelin basic protein. The inhibitory effects of okadaic acid and the microcystin analogues were determined by preincubation of the enzymes with serial dilutions of each compound for 10 min before the addition of the radiolabeled substrate. [$^{33}$P]ATP-labeled myelin basic protein was added to the reaction (final reaction volume, 50 μL) and immediately incubated at 30°C for 10 min. The reaction was stopped by the addition of 200 μL of ice-cold 20% trichloroacetic acid and incubated for a further 10 min on ice. The precipitated protein was pelleted by centrifugation at 12,000 × *g* at 4°C for 5 min, after which 200 μL of the supernatant was carefully removed, and the amount of released $^{33}$P was determined by liquid scintillation counting. The data were normalized to a duplicate control reaction done in the absence of the phosphatases. $IC_{50}$ was calculated as the concentration of drug that inhibited the release of $^{33}$P compared with an uninhibited control reaction.

### Intracellular Protein Phosphatase Analysis

To determine the effects of the microcystins on the activity of the intracellular phosphatases in the transiently transfected HeLa cells, cell lysates were prepared as follows. Forty-eight hours following transfection, HeLa cells transfected with either pIRESneo2, OATP1B1, or OATP1B3 were treated with microcystin analogues and okadaic acid at approximately $IC_{90}$ concentrations for 6 h. The cells were subsequently washed in ice-cold PBS, and 500 μL of the phosphatase assay buffer containing 80 μL/mL of Complete Protease Inhibitor cocktail was added to each well. The cells were immediately scraped, collected in 1.5 mL microcentrifuge tubes, and freeze/thawed twice in dry ice/room temperature water. The cells were further lysed by repeated pipetting (×10) and immediately centrifuged at 12,000 × *g* for 10 min at 4°C. The remaining supernatant was collected and frozen at −80°C. The protein concentration of the cell lysates was measured using the Bio-Rad protein assay. To determine the levels of phosphatase inhibition in the microcystin-treated cells, 20 ng of cellular protein was incubated in phosphatase assay buffer in the presence of [$^{33}$P]ATP-labeled myelin basic protein as described above. The results are presented as the percent of total phosphatase activity relative to untransfected untreated HeLa cells.

### Cellular and Nuclear Morphology Studies

HeLa cells were transiently transfected with OATP1B1 or empty pIRESneo2 as described above. Forty-eight hours after transfection, the cells were treated with 10 nmol/L microcystin LR for 6 h. Floating and adherent cells were subsequently pooled and washed once with ice-cold PBS. Cells were then either fixed in Carnoy's fixative, or live cells were immediately analyzed by flow cytometry, side scatter (granularity) versus forward scatter (relative size), to determined changes in gross cell morphology relative to a control (untreated) population. Flow cytometry was done using a BD FACSCalibur system (BD Biosciences, Franklin Lakes, NJ). Fixed cells were stained with Hoechst 33258 (1 μg/mL dissolved in PBS), and changes in nuclear/DNA morphology were determined by fluorescent confocal microscopy. Bright-field and fluorescent images were taken under a ×40 oil immersion objective using a confocal Leica DM IRBE inverted microscope equipped with a Spectra-Physics 2 photon sapphire/titanium laser and transmitted light detector for differential interference contrast and phase microscopy.

## Results

### OATP1B3 Expression Is Increased in NSCLC Tumors Relative to Adjacent Nonmalignant Tissue

We analyzed the expression of 19 drug and vitamin transport genes in 19 pairs of NSCLC tumors and surrounding nonmalignant tissue obtained from the National Cancer Institute Cooperative Human Tissue Network. RNA extracted from tumors was analyzed for transporter gene expression using quantitative real-time PCR, and the results were normalized to the expression of *β-actin*. The ratio between the expression in tumor compared with adjacent nonmalignant tissue for each paired sample was calculated, and the median value for the series of tumor/tissue pairs for each gene is presented in Table 1.

The mRNA of only one gene (*OATP1B3*) was found to be up-regulated by a median value of 6.4-fold in lung tumors compared with surrounding normal tissue, whereas all of the other transport genes showed little increase in expression. A number of genes did show a decrease in lung tumor expression, with the transporters *OATP2A1, OCT2, OCT3, OCTN1*, and *THTR2* all showing >3-fold drop in expression. The decrease RNA levels of *THTR2* in this series is consistent with our previous study of *THTR2* RNA levels in NSCLC, which used a different set of NSCLC tumor/tissue pairs and a different methodology (hybridization of labeled probes to a cDNA array; ref. 16), and which also found a decrease in *THTR2* RNA levels in NSCLC tumors relative to adjacent nonmalignant tissue.

To further illustrate the changes in expression between tumor and normal lung tissue, representative scatter plots for *OATP1B1* (*A*), *THTR2* (*B*), and *OATP1A2* (*C*) are shown in Fig. 1. The solid line represents the median value presented in Table 1; the dotted line represents a reference sample showing the expression in a normal tissue known to express each gene. Of particular interest is the increased

**Table 1. Ratio of transporter gene expression in lung tumors compared with normal surrounding tissue**

| Transporter | Gene symbol | Tumor/normal ratio |
|---|---|---|
| OAT1 | *SLC22A6* | 0.62 |
| OAT2 | *SLC22A7* | 0.90 |
| OAT3 | *SLC22A8* | 1.17 |
| OAT4 | *SLC22A11* | 1.11 |
| OATP1A2 | *SLC21A3* | 1.28 |
| OATP1B3 | *SLC21A8* | 6.38 |
| OATP1C1 | *SLC21A14* | 0.68 |
| OATP2A1 | *SLC21A2* | 0.18 |
| OATP2B1 | *SLC21A9* | 0.47 |
| OATP3A1 | *SLC21A11* | 0.95 |
| OATP4A1 | *SLC21A12* | 1.24 |
| OCT1 | *SLC22A1* | 0.81 |
| OCT2 | *SLC22A2* | 0.36 |
| OCT3 | *SLC22A3* | 0.33 |
| OCTN1 | *SLC22A4* | 0.25 |
| OCTN2 | *SLC22A5* | 0.81 |
| RFC1 | *SLC19A1* | 0.78 |
| THTR1 | *SLC19A2* | 0.67 |
| THTR2 | *SLC19A3* | 0.35 |

NOTE: Relative expression levels of 19 drug and vitamin transport genes in 19 pairs of NSCLC tumors compared with surrounding nonmalignant tissue, obtained from the National Cancer Institute Cooperative Human Tissue Network. DNase-treated mRNA was isolated from tissues as described in Materials and Methods. Following cDNA synthesis, expression levels of each gene were analyzed using quantitative real-time PCR. *β-Actin* levels were used to normalize the expression, and data are presented as the ratio of the median tumor expression compared with the median of the paired normal tissue.

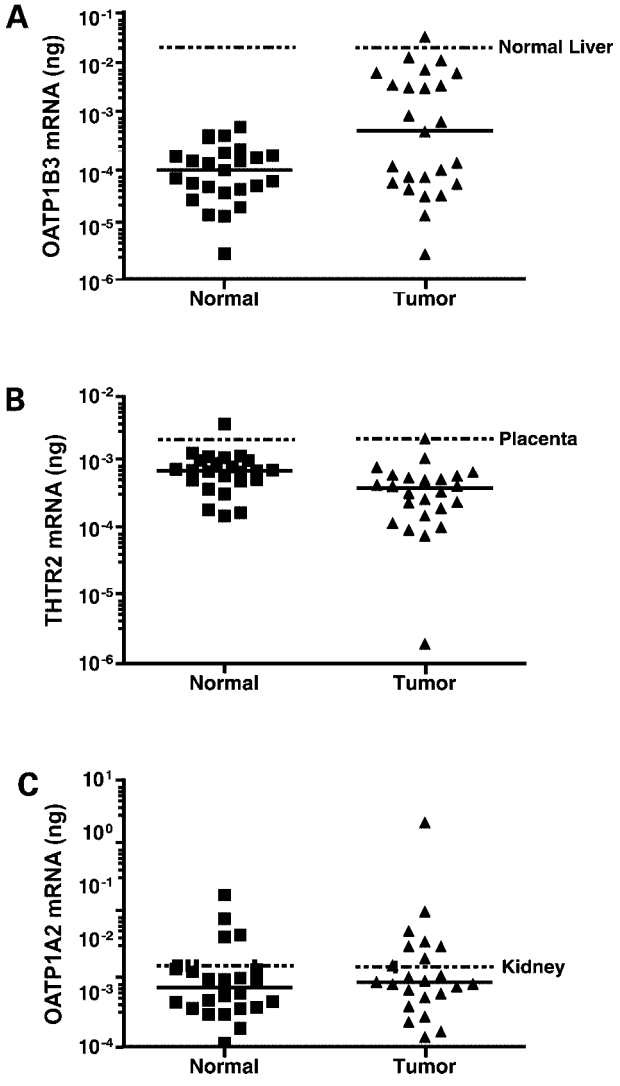


**Figure 1.** Scatter plots displaying the expression levels of *OATP1B3* (**A**), *THTR2* (**B**), and *OATP1A2* (**C**) for each of the 19 individual lung tumors (▲) and normal tissue (■) pairs. *Solid line,* median of the data set; *dotted lines,* expression level in a reference sample from a normal tissue known to express the gene of interest. The data presented are expression level of each individual sample following normalization to *β-actin*.

expression of *OATP1B3* in a number of the lung tumor samples (Fig. 1A), which is comparable with the expression level of *OATP1B3* in normal liver.

### HeLa Transient Transfection Model Shows Equivalent Levels of Transporter Expression to Liver and PP1 and PP2A Expression Suitable for the Study of Microcystins

To explore whether OATP1B3 expression could confer sensitivity to its toxic substrates (e.g., microcystin), and thus be exploited as potential target in lung cancer, hepatic cancer, and other malignancies, a transgenic model of *OATP1B3* and the closely related gene *OATP1B1* was needed. Because of their relative ease of transfection and capacity to express transgenes, we performed initial investigations in HeLa cells as a proof-of-principle. Exponentially growing HeLa cells were transiently transfected with the expression plasmids containing the *OATP1B1* and *OATP1B3* cDNA inserts, or a plasmid without a cDNA insert (vector control). To confirm the expression level of the cloned cDNAs and to determine the approximate level of expression in the transfected HeLa cells relative to both control cells and normal liver cDNA, we did real-time PCR as shown in Fig. 2A and B. These studies show that the RNA levels in the transient transfection system approximate the levels seen in normal adult liver. Of significant interest, we observed that the hepatic-derived cell lines have lost expression of these transporters in comparison with normal liver, and lung cancer cell lines also have either very low or undetectable levels of RNA expression of these transporter genes.

Because microcystins are known substrates of OATP1B1 and OATP1B3 and are also acknowledged inhibitors of PP1 and PP2A (it was important to show that HeLa, lung, and hepatic cancer cells express PP1 and PP2A), Western blot analysis was done using antibodies directed against PP1 and PP2A (Fig. 2C and D). This study shows that both phosphatases are present in HeLa cells, indicating that HeLa cells would make an appropriate *in vitro* model system. The studies also show that PP1 and PP2A are present in cell lines created from tumors that are known to express OATP1B1 and/or OATP1B3: the lung cancer cell lines A549, NCI-H460, and NCI-H23 and the hepatocellular carcinoma cell lines SNU-449, SNU-182, and Hep3B. The SV40 immortalized hepatic cell lines THLE-2 and THLE-3 are also shown.

### HeLa Expression Models Exhibit Functional Activity and Confers Increased Sensitivity to Microcystin LR and Other Natural Microcystin Analogues

To determine whether the RNA expression in transiently transfected HeLa cells resulted in functional activity of the transport genes, we studied the uptake of radiolabeled BQ123, a substrate for both OATP1B1 and OATP1B3, and cholecystokinin octapeptide (CCK8), a substrate specific for OATP1B3 only. As shown in Fig. 3, gene-specific uptake of BQ123 can be seen in both OATP1B1- and OATP1B3-transfected cells (Fig. 3A), and OATP1B3-specific uptake of cholecystokinin octapeptide can be seen in OATP1B3-transfected cells (Fig. 3B). In both cases, uptake activity was inhibited by an excess of bromosulfophthalein (BSP; 50 μmol/L), a known competitive inhibitor of these transporters. These studies show that the functional activity of the cloned transfected genes is consistent with the previously reported substrate profile of these transporters (14). To determine whether the functional expression of OATP1B1 and OATP1B3 results in change sensitivity to microcystin LR, we exposed the transfected HeLa cells to microcystin LR in a 72-h growth inhibition assay. As can be seen in Fig. 3C, the $IC_{50}$ for microcystin LR in OATP1B1 cells was $5 \pm 1$ nmol/L, and the $IC_{50}$ for OATP1B3 cells was $39 \pm 8$ nmol/L, whereas the toxicity in the control cells was not reached at 10 μmol/L. Similar results were seen using the clonogenic assay (Fig. 3D), which again identified the differential sensitivity for microcystin LR between

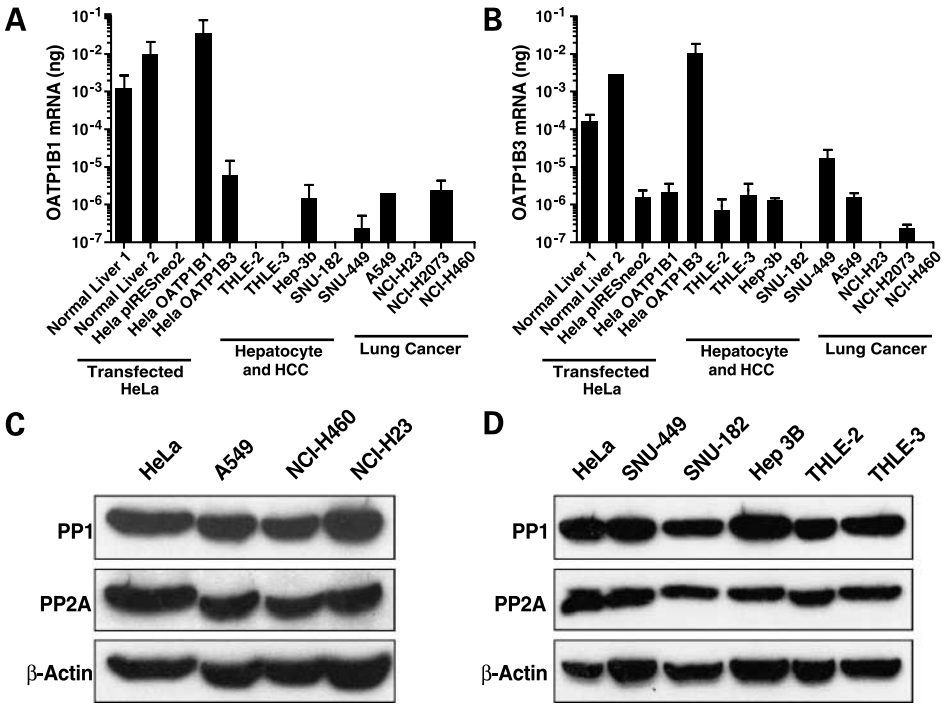


**Figure 2.** Expression levels of *OATP1B1* and *OATP1B3* in normal liver, transfected HeLa cells, immortalized hepatocyte cell lines, hepatocellular carcinoma cells (*HCC*), and lung cancer cell lines. Cells were collected, and DNase-treated RNA was isolated as described in Materials and Methods. Following cDNA synthesis, expression levels of *OATP1B1* (**A**) and *OATP1B3* (**B**) were analyzed using quantitative real-time PCR; *β-actin* levels were used to normalize the expression. *Columns,* mean of duplicate analysis; *bars,* SD. Protein phosphatases PP1 and PP2A are ubiquitously expressed in all of the cell lines. Whole-cell lysates of lung cancer (**C**) and hepatocellular carcinoma (**D**) cell lines, with HeLa cells used as a reference, were taken, and equal amounts (25 μg per lane) of total protein were separated on a 10% SDS-PAGE gel, transferred to nitrocellulose, and immunoblotted for both PP1 and PP2A as described in Materials and Methods. β-Actin was used to show equal loading.

OATP1B1 ($LC_{50}$ = 2 nmol/L) and OATP1B3 ($LC_{50}$ = 30 nmol/L), with no toxicity seen in the vector alone (pIRESneo2) cells. These results show the potential selective toxicity that the expression of these transporter genes confers on HeLa cells after exposure to microcystin LR.

To determine whether microcystin toxicity can be specifically inhibited in OATP1B1- and OATP1B3-transfected cells, we did a growth inhibition study with microcystin LR in the presence or absence of bromosulfophthalein. As can also be seen in Fig. 3C, bromosulfophthalein significantly shifted the growth inhibition curve to the right, increasing the $IC_{50}$ for both OATP1B1- and OATP1B3-transfected cells from 5 and 39 nmol/L, respectively, to ~5 μmol/L, further confirming the role of OATP1B1 and OATP1B3 uptake in microcystin LR toxicity. To further understand the activity of microcystin LR, we exposed OATP1B1-transfected HeLa cells to microcystin LR for 1, 6, and 72 h (Fig. 3E). A 1-h exposure was found to be less active, whereas the 6-h exposure was similar to 72 h; identical results were obtained with OATP1B3-transfected cells (data not shown). This result shows that toxic effects of microcystin LR are rapid, reaching a maximum effect after only a 6 h incubation.

We subsequently examined four other microcystin analogues using growth inhibition assays in the transfected HeLa cells to determine whether there was evidence that different structural analogues had greater potency or selectivity than microcystin LR. We also used okadaic acid, the classic phosphatase inhibitor that was not thought to have selective uptake requirements, as a positive control. As shown in Table 2, two of the analogues examined (microcystin LF and microcystin LW) showed greater cytotoxic potency than microcystin LR, with both showing $IC_{50}$ values in both of the gene-transfected cell lines of <1 nmol/L, with no evidence of toxicity in the vector only–transfected cells at concentrations up to 1 μmol/L. Microcystin RR exhibited much less potent cytotoxicity, with an $IC_{50}$ of 3.8 ± 2.3 and 0.58 ± 0.40 μmol/L for OATP1B1- and OATP1B3-transfected cells, respectively. Still, the transporter gene expression increased cytotoxicity of microcystin RR, with the vector-transfected cells not showing any cytotoxicity at concentrations up to 10 μmol/L. Both microcystins LR and RR showed differential toxicity between the cells transfected with either OAPT1B1 or OATP1B3. These data show that structural variation in the microcystin analogues provides a degree of transporter selectivity.

### Microcystins Show Both Potent and Differential Inhibition of Protein Phosphatases

The *in vitro* analysis of microcystin inhibition on purified PP1 and PP2A phosphatases is also shown in Table 2. The values determined are consistent with previously reported $K_i$ values for microcystin LR and okadaic acid. The reported $K_i$ values for microcystin-LR against PP1 and PP2A are 0.06 to 6 nmol/L and <0.01 to 2 nmol/L, respectively (17). Okadaic acid has a reported $IC_{50}$ of 60 to 500 nmol/L for PP1 and 15 to 70 nmol/L for PP2A (18).

Further evidence for the importance of selective phosphatase inhibition in cytotoxicity is provided in Fig. 4, which shows the correlation between the data in Table 2. Figure 4A and B shows the relationship between the growth inhibition $IC_{50}$ for the microcystin analogues and the *in vitro* enzyme inhibition $IC_{50}$ of PP2A and PP1, respectively, where microcystin LR is represented by □ (excluded from the linear regression analysis). In Fig. 4A,

the near-linear relationship between HeLa growth inhibition and PP2A enzyme inhibition ($r^2 > 0.99$) of four microcystin analogues (●) suggests that the activity of these analogues in the HeLa cells is related more to PP2A inhibition than PP1 (Fig. 4B). Similar results were found in the HeLa cells transfected with OATP1B3 (data not shown). The relation between cytotoxicity and PP2A inhibition is further supported by the observation that the $IC_{50}$ values of the analogues for growth inhibition and PP2A enzyme inhibition are both in the same subnanomolar range. The results with okadaic acid (■) further support this conclusion.

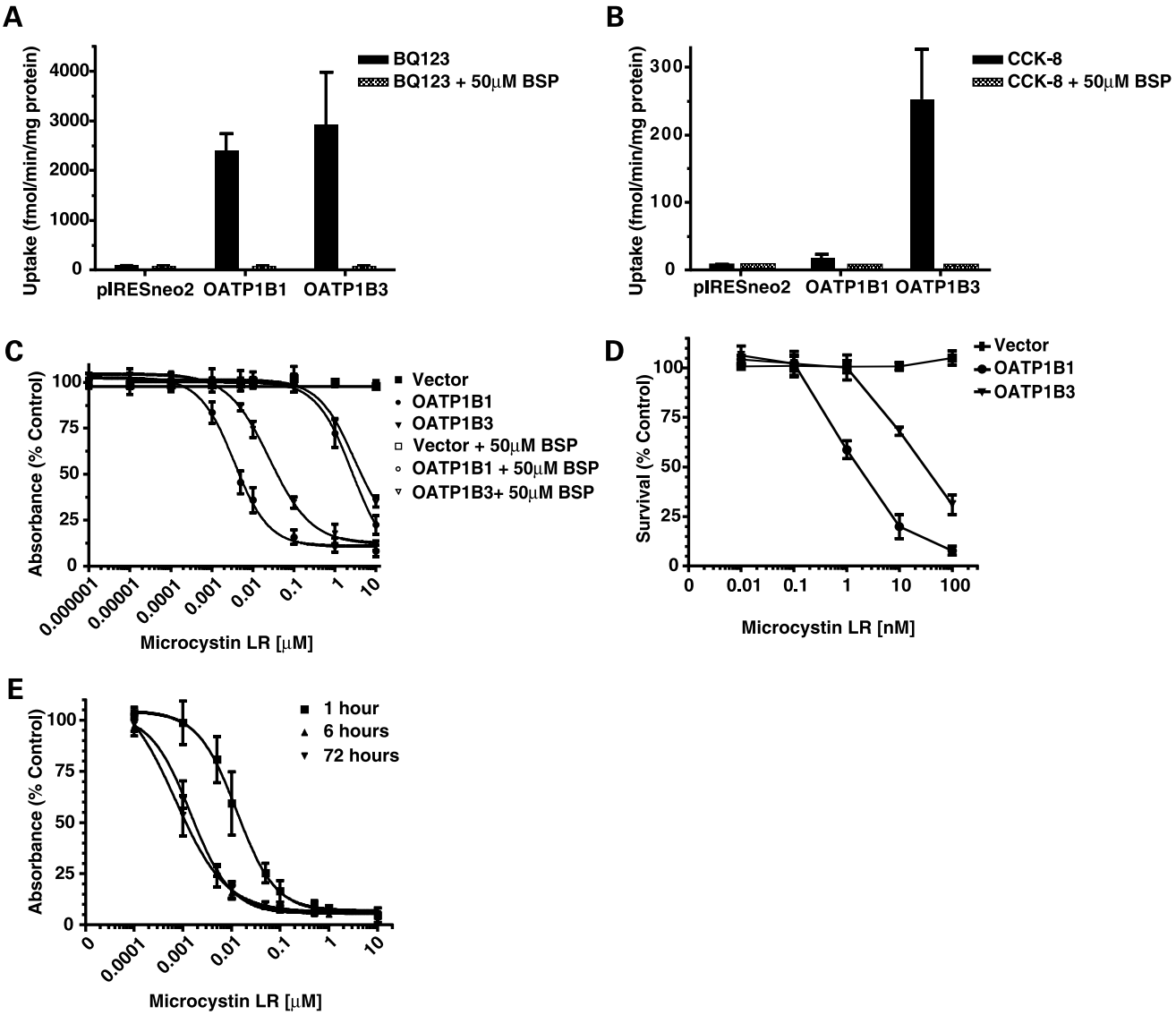


**Figure 3.** Uptake of radiolabeled OATP1B1 and OATP1B3 substrates. Cells were seeded in six-well plates, transfected, and assayed for uptake 48 h later as described in Materials and Methods. (**A**) [$^3$H]BQ123 (0.5 μmol/L for 30 min), a substrate of both OATP1B1 and OATP1B3, and (**B**) [$^3$H]cholecystokinin octapeptide (*CCK-8*; 5 nmol/L for 10 min), a substrate specific for OATP1B3, were also co-incubated in the presence of the competitive substrate bromosulfophthalein (*BSP*; 50 μmol/L). *Columns,* mean of three replicate experiments; *bars,* SD. **C,** growth inhibition of OATP1B1-transfected (○ and ●) and OATP1B3-transfected HeLa cells (▼ and ▽) and mock-transfected HeLa cells (■ and □) exposed to microcystin LR in the presence (○, ▽, and □) and absence (●, ▼, and ■) of the uptake inhibitor bromosulfophthalein. The cells were seeded in 96-well plates 24 h following transfection with either the control plasmid pIRESneo2, OATP1B1, or OATP1B3 containing vectors. Twenty-four hours after seeding, the cells were exposed to a range of microcystin LR concentrations for 72 h with or without the competitive transport substrate bromosulfophthalein (50 μmol/L). Growth inhibition was determined using the sulforhodamine B dye assay as described in the Materials and Methods, and data are presented as the percentage of untreated control growth. *Points,* mean of three replicate experiments; *bars,* SD. **D,** clonogenic survival of HeLa cells transfected with pIRESneo2 (■), OATP1B1 (●), or OATP1B3 (▼) following a 72-h exposure to microcystin LR. *Points,* mean of three replicate experiments; *bars,* SD. **E,** growth inhibition of OATP1B1-transfected HeLa cells exposed to microcystin LR for 1 h (■), 6 h (▲), and 72 h (▼). Growth inhibition was determined using the sulforhodamine B dye assay, and data are presented as the percentage of untreated control growth. *Points,* mean of three replicate experiments; *bars,* SD.

**Table 2. Microcystin analogue growth inhibition and protein phosphatase enzyme inhibition**

| Microcystin analogue | Growth inhibition | | | Enzyme inhibition | |
|---|---|---|---|---|---|
| | pIRESneo2, $IC_{50}$ (nmol/L) | OATP1B1, $IC_{50}$ (nmol/L) | OATP1B3, $IC_{50}$ (nmol/L) | PP1, $IC_{50}$ (nmol/L) | PP2A, $IC_{50}$ (nmol/L) |
| LR | >10,000 | 5 ± 51 | 39 ± 8 | 1.4 ± 0.3 | 0.18 ± 0.01 |
| LF | >1,000 | 0.4 ± 0.1 | 0.9 ± 0.9 | 2.2 ± 1.5 | 0.30 ± 0.01 |
| LW | >1,000 | 0.3 ± 0.1 | 0.5 ± 0.4 | 3.1 ± 0.3 | 0.24 ± 0.02 |
| RR | >10,000 | 3,800 ± 2,300 | 580 ± 400 | 6.9 ± 0.01 | 22.0 ± 7.0 |
| YR | >1,000 | 90 ± 20 | 45 ± 30 | 18.0 ± 6.0 | 3.3 ± 0.14 |
| Okadaic acid | 7.8 ± 1.5 | 2.2 ± 0.6 | 3.0 ± 1.2 | 90 ± 17 | 0.40 ± 0.18 |

NOTE: Growth inhibition was determined in plasmid transfected HeLa cells. Cells were seeded into 96-well plates 24 h following transfection with control plasmid (pIRESneo2), *OATP1B1*, or *OATP1B3* containing vectors and, 24 h later, were exposed to a range of microcystin concentrations for a further 72 h. Growth inhibition was determined using the sulforhodamine B dye assay as described in Materials and Methods. The $IC_{50}$ data presented in the table represent the concentration at which the absorbance is 50% of the untreated control wells, $IC_{50}$ was determined by nonlinear regression (variable slope) analysis using the GraphPad Prism software. Phosphatase enzyme inhibition was determined using purified PP1 and PP2A enzyme. Enzyme was incubated with the microcystins at a range of concentrations for 10 min before the addition of [$^{33}$P]ATP-labeled myelin basic protein. The dephosphorylation reaction was allowed to proceed for 10 min, after which the reaction was stopped with trichloroacetic acid, and released $^{33}$P was determined by liquid scintillation counting as described in Materials and Methods. $IC_{50}$ was determined by nonlinear regression (variable slope) analysis using the GraphPad Prism software and represents the concentration at which the release of $^{33}$P was inhibited by 50% compared with the untreated enzyme control reaction. All data are presented as the mean ± SD of ≥3 replicate experiments.

We measured global phosphatase inhibition in the transfected HeLa cells exposed to approximately equitoxic ($IC_{90}$) concentrations of microcystins to further examine the relationship between the cytotoxic effects and protein phosphatase inhibition. In these studies, OATP1B3-transfected HeLa cells and empty vector control cells were exposed for 6 h to the microcystins at approximately equitoxic concentrations, and phosphatase activity in the cellular cytosol was then measured. As can be seen in Fig. 4C, total phosphatase inhibition does not directly correspond to cytotoxicity. For example, at a dose of ~2-fold greater than the cytotoxic $IC_{50}$ in OATP1B3-transfected HeLa cells, microcystin LF and LW (1 nmol/L) had no discernible effect on total phosphatase activity. At a similar equitoxic dose, microcystin LR (10 nmol/L) decreased total phosphatase activity by ~30% in OATP1B1-transfected cells. However, microcystin RR (1 μmol/L) decreased total phosphatase activity by 90%. These results suggest that specific phosphatase inhibition, not global inhibition, is related to cytotoxicity. These results also suggest that at higher concentrations, microcystins may have inhibitory effects on other phosphatases.

### Cell Death Induced by Microcystin LR Is Rapid

Figure 5 displays the results of microcystin LR induced cell death after a 6-h exposure. Using confocal microscopy and changes in cell morphology shown by flow

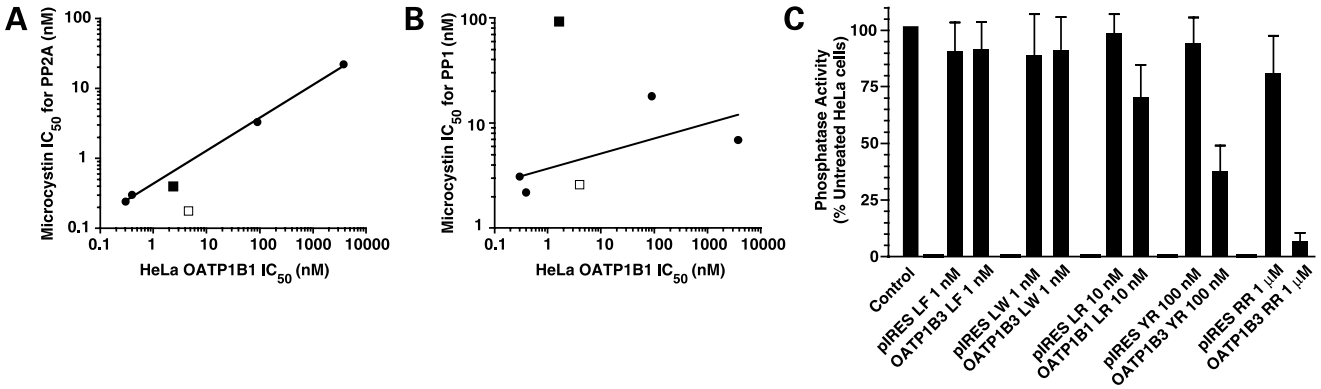


**Figure 4.** Correlations between growth inhibition and *in vitro* enzyme inhibition (data from Table 2). The relationship between the growth inhibition $IC_{50}$ for the microcystin analogues and the *in vitro* enzyme inhibition $IC_{50}$ of PP2A (**A**) and PP1 (**B**). ●, microcystin analogues LW, LF, RR, and YR. □, microcystin LR; ■, okadaic acid. The linear regression analysis was done using the GraphPad Prism software. **C,** inhibition of total phosphatase activity in transfected HeLa cells exposed to equitoxic concentrations ($IC_{90}$) of the microcystin analogues. Intracellular phosphatase enzyme inhibition was determined using whole-cell lysates prepared from transfected HeLa cells exposed to $IC_{90}$ concentrations of the microcystin analogues for 6 h as described in Materials and Methods. Twenty nanograms of cellular protein were incubated in phosphatase assay buffer in the presence of [$^{33}$P]ATP-labeled myelin basic protein for 10 min, after which the reaction was stopped with trichloroacetic acid, and released $^{33}$P was determined by liquid scintillation counting. The data are presented as the percentage phosphatase activity relative to untransfected and untreated HeLa cells. *Points/columns,* mean of three replicate experiments; *bars,* SD.

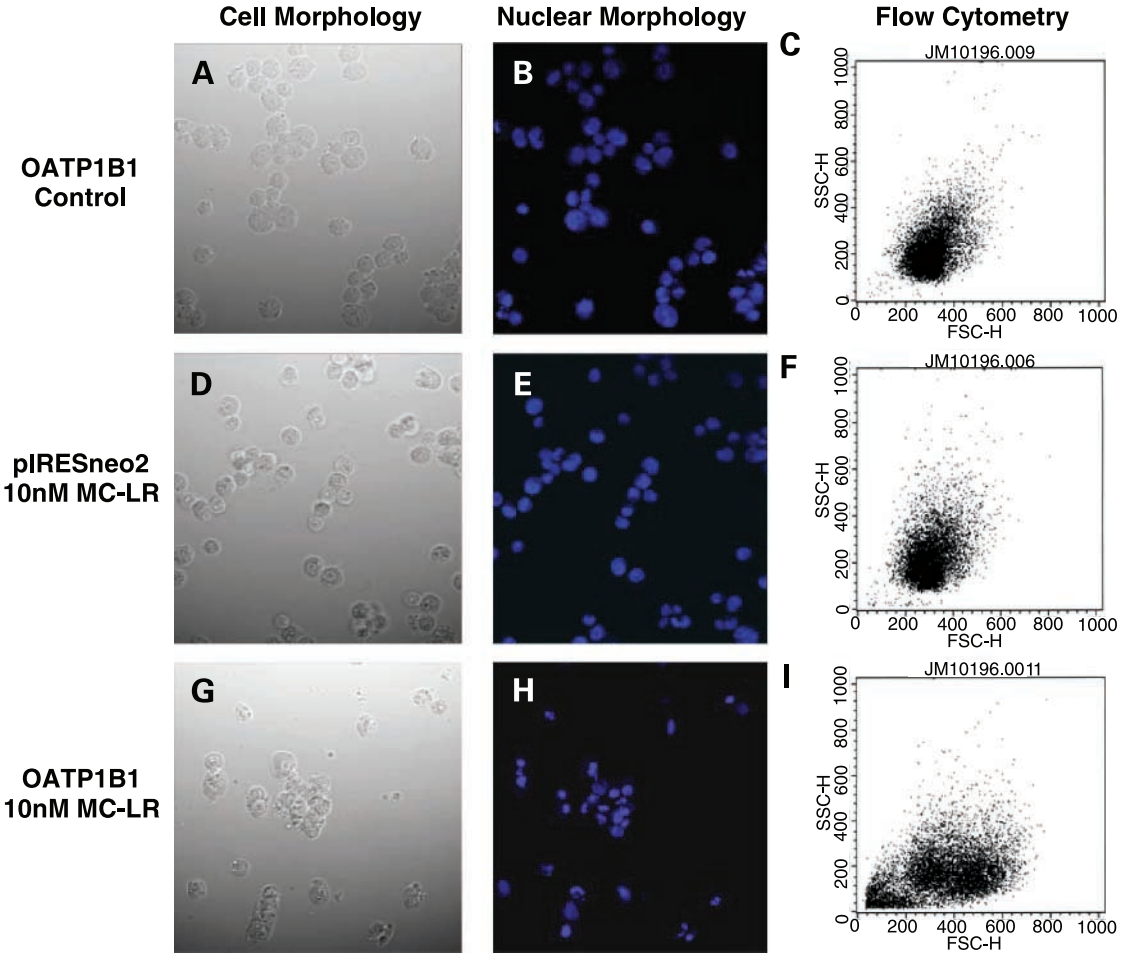


**Figure 5.** Cell death induced by 10 nmol/L microcystin LR (*MC-LR*) 6 h after treatment. Untreated OATP1B1-transfected HeLa cells (**A**–**C**), 10 nmol/L treated vector control (pIRESneo2)–transfected HeLa cells (**D**–**F**), and 10 nmol/L treated OATP1B1-transfected HeLa cells (**G**–**I**). Bright-field images used to visualize cellular morphology (**A, D,** and **G**). Fluorescent images showing Hoechst 33258 stain to visualize nuclear morphology and DNA condensation (**B, E,** and **H**), Flow cytometry plots of side scatter (*SSC*) versus forward scatter (*FSC*) displaying the changes in cell size and the formation of cell fragments (**C, F**, and **I**).

cytometry, we have identified that exposure to microcystin LR induced rapid changes in cell and nuclear morphology. Initial morphologic changes are rapid detachment from the culture surface, which occurs within the first hour of exposure (data not shown). By 6 h, microcystin LR–treated OATP1B1-expressing cells display membrane blebbing (Fig. 5G), and massive cellular fragmentation can be detected using flow cytometry (Fig. 5I). Using Hoechst 33258 DNA stain, we also identified extensive chromatin condensation and fragmentation (Fig. 5H) following a 6-h microcystin LR exposure. Control (pIRESneo2) transfectants similarly treated with 10 nmol/L microcystin LR showed no changes in cellular morphology (Fig. 5D and F) and nuclear condensation (Fig. 5E), similar to the untreated OATP1B1-transfected control (Fig. 5A–C), further supporting the evidence that microcystins require a transport mechanism for cellular uptake and toxicity. Taken together, these data show that once microcystin LR gains entry into cells, it acts rapidly, causing morphologic changes that are indicative of cell death.

## Discussion

The observation that microcystin LR and its analogues show potent growth inhibitory and cytotoxicity activity in OATP1B1- and OATP1B3-transfected cells in comparison with control cells indicates both that the expression of these genes can impart selective sensitivity of cancer cells to cytotoxic substrates, and that phosphatase inhibition may be a valid target for anticancer drug development. Furthermore, the lack of activity of microcystin LR in the control HeLa cells shows that the stumbling block for developing microcystins as anticancer agents may be that these phosphatase inhibitors have difficulty gaining intracellular access in standard *in vitro* cytotoxicity models. This potential difficulty is supported by both our observations and those of others, that even hepatic-derived cell lines do

not reflect the level of transporter gene expression observed in the tissue and tumors of origin. In the case of *OATP1B1*, we found no detectable expression in any of the hepatocellular carcinoma cells or immortalized hepatocyte cell lines. In the case of *OATP1B3*, the level of mRNA expression in hepatocellular carcinoma cells and hepatocyte cell lines was at the limit of detection and orders of magnitude lower than the expression levels seen in normal adult liver. In particular, the widely used Hep3B cell line does not express OATP1B1, and the level of OATP1B3 is orders of magnitude lower than the levels measured in normal liver. In addition, another widely used model of hepatocellular carcinoma (the HepG2 cell line) also does not express either transporter (7). Similarly, the level of RNA expression in lung cancer cell lines is also low, although direct measurement of RNA levels in lung tumor tissue showed increased expression relative to normal lung tissue, with the increased expression in the tumor samples being similar to that of a normal liver reference. In the case of both transporters, the constitutive levels in all of the hepatic cell lines was at the level of the untransfected HeLa cells, whereas the transfected HeLa cells had mRNA levels similar to the levels measured in normal liver. We have seen a similar down regulation in cell lines versus tumors in the case of another membrane transporter, OCT6 (19). Supporting our observations, the loss of microcystin sensitivity in freshly isolated trout and murine hepatocytes was observed to coincide with the rapid loss of OATP transporter gene expression when the hepatocytes are maintained in cell culture (20). Thus, down-regulation of membrane transport that occurs in adaptation to *in vitro* growth conditions has the potential to limit the interpretation of cell culture–based screening systems for polar cytotoxins that depend on specific mechanisms of drug uptake.

Because transporter gene expression in tumors cannot be extrapolated from cell lines, direct measurement of tumor gene expression is required. However, studies quantifying mRNA levels in tumors also have limitations in interpretation. It is important to acknowledge that whereas the data show increased expression of *OATP1B3* mRNA in lung tumors, these data must be interpreted with caution, as the mRNA levels do not necessarily reflect either protein expression or function. The actual sensitivity of NSCLC tumors to microcystin analogues, and of microcystin uptake in NSCLC tumors relative to hepatocytes, are important questions to be explored with xenograft models.

Significant obstacles must be overcome in the development of microcystin analogues as potential therapeutic agents. Most importantly, a strategy must be devised to create a useful therapeutic window for microcystins, in which the potent hepatic toxicity of these agents is overcome. The microcystin concentrations that produced cytotoxicity in the transfected HeLa cells in our study, in the subnanomolar range for microcystin LF and microcystin LW, seem to be significantly less than the doses required for hepatic toxicity. In mice given a sublethal dose of microcystin LR (35 μg/kg), the peak plasma concentration achieved was 428 nmol/L (21) compared with the $IC_{50}$ values of 5 and 39 nmol/L for microcystin LR in OATP1B1- and OATP1B3-transfected HeLa cells, respectively (Table 2). In addition, microcystin rapidly accumulates in the liver, with 70% of the total dose accumulating by 30 min after the injection (21). We have shown that the cytotoxic activity of microcystin LR is rapid, and although maximal activity was not seen until 6 h, a 1-h exposure showed significant levels of activity (Fig. 3E).

Our data strongly suggest that microcystin cytotoxicity in HeLa cells is related to specific PP2A inhibition. We found no correlation between global phosphatase inhibition and cytotoxicity. The similar concentrations for PP2A enzyme inhibition and growth inhibition and the linear correlation between the growth $IC_{50}$ and the enzyme $IC_{50}$ for microcystin analogues both suggest that specific PP2A inhibition is related to the toxic effect.

The high concentration of microcystin in the liver achieved with a sublethal dose (21) suggests that hepatocytes may differ from cancer cells in the mechanism of microcystin toxicity. First, hepatic lethality may be related to an intracellular target other than PP2A. One such target may be aldehyde dehydrogenase II, an enzyme involved in acetaldehyde detoxification and prevention of free radical formation, which was recently identified as a microcystin target from a peptide fragment that physically associated with microcystin LR using phage display methodology (22). Another potential microcystin target is the β subunit of ATP-synthase, which was shown to be a microcystin-binding protein using an anti-microcystin antibody-affinity purification column (23).

Second, reports of microcystin cytotoxicity in nonmalignant cells, in which a significantly higher dose is required for toxicity, is seemingly related to formation of reactive oxygen species (24) and resultant DNA damage (25). In lymphocytes *in vitro*, the mechanism of microcystin toxicity was associated with free radical formation; in those studies, cells were exposed to micromolar concentrations of microcystin LR (26, 27), in comparison with the subnanomolar range in the transfected HeLa cells.

Third, phosphatase inhibition may have different effects in tumor cells versus normal cells. Although protein phosphatases have tumor suppressor properties, phosphatases have been also been reported to promote cell growth and survival (9, 10). The cytotoxic effect of phosphatase inhibition may depend upon the reliance of a particular cell on the activity of specific kinases, which are often abnormally regulated in cancer. For example, the phosphatase inhibitor okadaic acid has been shown to induce apoptosis in a variety of cell lines, with increased sensitivity reported in cells carrying mutated Ras (28). Okadaic acid also induced apoptosis in malignant glioma cells, in studies that suggested an integral role for ERK and c-Jun $NH_2$-terminal kinase (JNK kinase) in promoting cell death (29). Rapid apoptosis has also been seen in primary hepatocytes following microinjection with both microcystin LR and nodularin, characterized by cytoplasmic shrinkage, chromatin condensation, membrane blebbing,

and procaspase-3 cleavage (30). Similarly, we have identified rapid cell death (within 6 h), although at a much lower concentration (10 nmol/L) than those used by Fladmark et al. (nodularin >250 μmol/L and microcystin LR >50 μmol/L).

Finally, in addition to potential differences in microcystin intracellular targets between hepatocytes and cancer cells, there are also numerous metabolic differences between the normal hepatocyte and the malignant cell, and these differences might be exploited to create a therapeutic window for microcystin toxins. Microcystin and the related toxic cyclic peptide nodularin seem to stimulate glutathione-dependent detoxification pathways in hepatocytes. Exposure of rat hepatocytes to sublethal concentrations of microcystin LR results in an acute increase in intracellular glutathione and an increase in the formation of reactive oxygen species (31). Significantly, addition of *N*-acetylcysteine to the culture medium, an agent that increases intracellular glutathione concentrations, decreased sensitivity of cultured rat hepatocytes to microcystic cyanobacteria extracts. Conversely, buthionine sulfoximine, an agent that decreases intracellular glutathione, increased the sensitivity of the cultured hepatocytes to the cyanobacteria extract (32). These studies suggest that glutathione may play a role in the *in vivo* hepatic detoxification of microcystins at high concentrations. In our HeLa cell model, neither *N*-acetylcysteine nor buthionine sulfoximine affected microcystin toxicity (data not shown).

In conclusion, therapeutic microcystin analogues may have the potential to exploit both differences in the mechanisms of toxicity and the availability of detoxification mechanisms in tumors versus normal hepatic tissue. The restricted hepatic expression of OATP1B1 and OATP1B3 would help to prevent toxicities to nonmalignant tissues other than liver, and the expression of these transporters in NSCLC and hepatocellular carcinoma suggests that these tumors could be targeted with transporter-specific cytotoxins. We are currently developing an *in vivo* model to address the potential of microcystins as antitumor agents targeted at OATP1B1- and OATP1B3-expressing tumors. Microcystins, as stable cyclic peptides with two variable amino acid positions, are attractive candidates for combinatorial synthesis, and the variation in potency between the first five microcystin analogues tested suggests that other analogues may be even more potent.

#### Acknowledgments

We thank Drs. Meier and Hagenbuch for the gift of OATP1B1 and OATP1B3 cDNAs in the vector pIRESneo2, Dr. Larry Matherly (Wayne State University) for technical advice, James Begley and Melissa Higdon for their assistance with the confocal microscopy, and Dr. Greg Bauman for his assistance with flow cytometry.

#### References

**1.** Taylor WP, Widlanski TS. Charged with meaning: the structure and mechanism of phosphoprotein phosphatases. Chem Biol 1995;2:713 – 8.

**2.** Cheng A, Dean NM, Honkanen RE. Serine/threonine protein phosphatase type 1gamma1 is required for the completion of cytokinesis in human A549 lung carcinoma cells. J Biol Chem 2000;275:1846 – 54.

**3.** MacKintosh C, Beattie KA, Klumpp S, Cohen P, Codd GA. Cyanobacterial microcystin-LR is a potent and specific inhibitor of protein phosphatases 1 and 2A from both mammals and higher plants. FEBS Lett 1990;264:187 – 92.

**4.** WHO. Cyanobacterial toxins: microcystin-LR. World Health Organization: guidelines for drinking-water quality. Geneva: WHO; 1998. p. 95 – 110.

**5.** Cui Y, Konig J, Nies AT, et al. Detection of the human organic anion transporters SLC21A6 (OATP2) and SLC21A8 (OATP8) in liver and hepatocellular carcinoma. Lab Invest 2003;83:527 – 38.

**6.** Hagenbuch B, Meier PJ. Organic anion transporting polypeptides of the OATP/SLC21 family: phylogenetic classification as OATP/SLCO superfamily, new nomenclature and molecular/functional properties. Pflugers Arch 2004;447:653 – 65.

**7.** Abe T, Unno M, Onogawa T, et al. LST-2, a human liver-specific organic anion transporter, determines methotrexate sensitivity in gastrointestinal cancers. Gastroenterology 2001;120:1689 – 99.

**8.** Janssens V, Goris J. Protein phosphatase 2A: a highly regulated family of serine/threonine phosphatases implicated in cell growth and signalling. Biochem J 2001;353:417 – 39.

**9.** Janssens V, Goris J, Van Hoof C. PP2A: the expected tumor suppressor. Curr Opin Genet Dev 2005;15:34 – 41.

**10.** Millward TA, Zolnierowicz S, Hemmings BA. Regulation of protein kinase cascades by protein phosphatase 2A. Trends Biochem Sci 1999; 24:186 – 91.

**11.** Messner DJ, Romeo C, Boynton A, Rossie S. Inhibition of PP2A, but not PP5, mediates p53 activation by low levels of okadaic acid in rat liver epithelial cells. J Cell Biochem 2006;99:241 – 55.

**12.** Yan Y, Shay JW, Wright WE, Mumby MC. Inhibition of protein phosphatase activity induces p53-dependent apoptosis in the absence of p53 transactivation. J Biol Chem 1997;272:15220 – 6.

**13.** Lin SS, Bassik MC, Suh H, et al. PP2A regulates BCL-2 phosphorylation and proteasome-mediated degradation at the endoplasmic reticulum. J Biol Chem 2006;281:23003 – 12.

**14.** Hagenbuch B, Meier PJ. The superfamily of organic anion transporting polypeptides. Biochim Biophys Acta 2003;1609:1 – 18.

**15.** Skehan P, Storeng R, Scudiero D, et al. New colorimetric cytotoxicity assay for anticancer drug screening. J Natl Cancer Inst 1990;82:1107 – 12.

**16.** Liu S, Stromberg A, Tai HH, Moscow JA. Thiamine transporter gene expression and exogenous thiamine modulate the expression of genes involved in drug and prostaglandin metabolism in breast cancer cells. Mol Cancer Res 2004;2:477 – 87.

**17.** Fujiki H, Suganuma M. Tumor promotion by inhibitors of protein phosphatases 1 and 2A: the okadaic acid class of compounds. Adv Cancer Res 1993;61:143 – 94.

**18.** Ishihara H, Martin BL, Brautigan DL, et al. Calyculin A and okadaic acid: inhibitors of protein phosphatase activity. Biochem Biophys Res Commun 1989;159:871 – 7.

**19.** Gong S, Lu X, Xu Y, Swiderski CF, Jordan CT, Moscow JA. Identification of OCT6 as a novel organic cation transporter preferentially expressed in hematopoietic cells and leukemias. Exp Hematol 2002;30: 1162 – 9.

**20.** Boaru DA, Dragos N, Schirmer K. Microcystin-LR induced cellular effects in mammalian and fish primary hepatocyte cultures and cell lines: a comparative study. Toxicology 2006;218:134 – 48.

**21.** Robinson NA, Pace JG, Matson CF, Miura GA, Lawrence WB. Tissue distribution, excretion and hepatic biotransformation of microcystin-LR in mice. J Pharmacol Exp Ther 1991;256:176 – 82.

**22.** Chen T, Cui J, Liang Y, et al. Identification of human liver mitochondrial aldehyde dehydrogenase as a potential target for microcystin-LR. Toxicology 2006;220:71 – 80.

**23.** Mikhailov A, Harmala-Brasken AS, Hellman J, Meriluoto J, Eriksson JE. Identification of ATP-synthase as a novel intracellular target for microcystin-LR. Chem Biol Interact 2003;142:223 – 37.

**24.** Ding WX, Nam Ong C. Role of oxidative stress and mitochondrial changes in cyanobacteria-induced apoptosis and hepatotoxicity. FEMS Microbiol Lett 2003;220:1 – 7.

**25.** Ding WX, Shen HM, Zhu HG, Lee BL, Ong CN. Genotoxicity of

microcystic cyanobacteria extract of a water source in China. Mutat Res 1999;442:69 – 77.

**26.** Lankoff A, Carmichael WW, Grasman KA, Yuan M. The uptake kinetics and immunotoxic effects of microcystin-LR in human and chicken peripheral blood lymphocytes *in vitro*. Toxicology 2004;204:23 – 40.

**27.** Lankoff A, Krzowski L, Glab J, et al. DNA damage and repair in human peripheral blood lymphocytes following treatment with microcystin-LR. Mutat Res 2004;559:131 – 42.

**28.** Rajesh D, Schell K, Verma AK. Ras mutation, irrespective of cell type and p53 status, determines a cell's destiny to undergo apoptosis by okadaic acid, an inhibitor of protein phosphatase 1 and 2A. Mol Pharmacol 1999;56:515 – 25.

**29.** Rami BG, Chin LS, Lazio BE, Singh SK. Okadaic-acid-induced apoptosis in malignant glioma cells. Neurosurg Focus 2003;14:e4.

**30.** Fladmark KE, Brustugun OT, Hovland R, et al. Ultrarapid caspase-3 dependent apoptosis induction by serine/threonine phosphatase inhibitors. Cell Death Differ 1999;6:1099 – 108.

**31.** Bouaicha N, Maatouk I. Microcystin-LR and nodularin induce intracellular glutathione alteration, reactive oxygen species production and lipid peroxidation in primary cultured rat hepatocytes. Toxicol Lett 2004;148:53 – 63.

**32.** Ding WX, Shen HM, Ong CN. Microcystic cyanobacteria extract induces cytoskeletal disruption and intracellular glutathione alteration in hepatocytes. Environ Health Perspect 2000;108:605 – 9.